International Journal of Nanomedicine

Dovepress
open access to scientific and medical research

Open Access Full Text Article

ORIGINAL RESEARCH

Apoptotic Extracellular Vesicles Derived from Human Umbilical Vein Endothelial Cells Promote Skin Repair by Enhancing Angiogenesis: From Death to Regeneration

Jinzhao Liu[1,2,*], Jia Dong[1,*], Xibo Pei[1,2]

[1]State Key Laboratory of Oral Diseases & National Center for Stomatology & National Clinical Research Center for Oral Diseases, West China Hospital of Stomatology, Sichuan University, Chengdu, Sichuan, 610041, People's Republic of China; [2]Department of Prosthodontics, West China Hospital of Stomatology, Sichuan University, Chengdu, Sichuan, 610041, People's Republic of China

*These authors contributed equally to this work

Correspondence: Jia Dong; Xibo Pei, Email scu2013dongjia@sina.com; xbpei@hotmail.com

Purpose: The promotion of angiogenesis is an effective strategy for skin wound repair. While the transplantation of endothelial cells has shown promise in vascularization, the underlying mechanism remains unclear. Recent studies have suggested that transplanted cells undergo apoptosis in a short period and release apoptotic extracellular vesicles (ApoEVs) that may have therapeutic potential.

Methods: In this study, we isolated ApoEVs from human umbilical vein endothelial cells (HUVECs) and characterized their properties. In vitro, we assessed the effects of ApoEVs on the proliferation, migration, and differentiation of endothelial cells and fibroblasts. In vivo, we investigated the therapeutic role of ApoEVs-AT in full-thickness skin wounds, evaluating wound closure rate, re-epithelialization, granulation tissue formation, vascularization, scar area, and collagen 3(Col3)/collagen 1(Col 1) ratio.

Results: ApoEVs derived from HUVECs displayed typical characteristics. In vitro, ApoEVs significantly enhanced the proliferation, migration, tube formation, and expression of angiogenic-related genes in endothelial cells and slightly promoted the proliferation and migration of fibroblasts. In vivo, ApoEVs improved the wound closure rate, re-epithelialization, the formation of granulation tissue, and vascularization. Besides, ApoEVs reduced scar formation, accompanied by an increase in the Col 3/ Col 1 ratio.

Conclusion: Given their abundant source and effectiveness, this study provided a novel approach for angiogenesis in tissue regeneration and deepened the understanding of from death to regeneration.

Keywords: apoptotic extracellular vesicles, human umbilical vein endothelial cells, skin regeneration, angiogenesis

Introduction

The skin serves as the primary barrier against external pathogens and any serious damage to it can impact human health and quality of life. Stimulating angiogenesis, the formation of new blood vessels is one of the most effective approaches for skin tissue repair.[1] Vascularization plays a critical role in facilitating nutrient delivery, maintaining oxygen levels, supporting cellular proliferation, and promoting tissue regeneration.[2] In previous studies, endothelial cells have been used for promoting vascularization in tissue repair and regeneration.[3–7] However, the safety and ethical concerns associated with live cells have posed significant limitations in clinical translational applications.[8] As a result, researchers have started investigating the mechanisms through which live cells exert therapeutic effects and have been searching for alternative solutions.

In recent years, it has become widely accepted that transplanted live cells release growth factors, cytokines, and extracellular vesicles, such as exosomes, through paracrine signaling to exert therapeutic effects.[9,10] However, growing studies have revealed that transplanted cells undergo extensive apoptosis within a short time, leading to the release of

Received: 13 October 2023
Accepted: 8 January 2024
Published: 16 January 2024

apoptotic extracellular vesicles (ApoEVs), which play a crucial role in therapeutic processes.[11–13] Therefore, it has been suggested that ApoEVs may significantly contribute to the therapeutic abilities of transplanted cells. Furthermore, studies have demonstrated that direct delivery of apoptotic mesenchymal stem cells (MSCs) or ApoEVs derived from apoptotic MSCs offers advantages over viable MSCs.[14,15]

Previous studies have primarily utilized bone marrow mesenchymal stem cells (BMSCs)[13,16–22] as the source of ApoEVs. Other cell types, including adipose mesenchymal stem cells (ASCs),[18] embryonic mesenchymal stem cells (ESCs),[23] umbilical cord mesenchymal stem cells (UMSCs),[23] and deciduous pulp stem cells,[24] as well as whole adipose tissue,[25] have also been selected in various studies. Among them, ApoEVs, isolated from BMSCs[22] and deciduous pulp stem cells,[24] were reported to regulate endothelial cell behavior and promote angiogenesis. Besides, ApoEVs, isolated from human embryonic stem cells (ESCs),[23] bone marrow mesenchymal stem cells (BMSCs),[26] and whole adipose tissue,[25] have been reported to promote skin wound healing.

Given the abundant availability of human umbilical vein endothelial cells (HUVECs) and the demonstrated effectiveness of their derivatives in multiple studies,[4,27–33] we hypothesized that ApoEVs isolated from apoptotic HUVECs could promote full-thickness skin wound healing by enhancing angiogenesis. To test this hypothesis, we adapted the method of preparing ApoEVs from MSCs and successfully isolated ApoEVs from HUVECs. We characterized these ApoEVs and evaluated their effects on the behavior of endothelial cells and fibroblasts in vitro. Furthermore, we investigated the therapeutic potential of ApoEVs in vivo by treating full-thickness skin wounds and assessing wound closure, re-epithelialization, granulation tissue formation, vascularization, scar reduction, and Col 3/Col 1 ratio.

Materials and Methods

Cell Culture

Primary human umbilical vein endothelial cells (HUVECs) were obtained from Procell Life Science & Technology (China). The characterization of morphology and endothelial cell marker, CD31, confirmed the purity of HUVECs (Supplementary Figure S1). HUVECs were cultured in endothelial cell growth medium (EGM, Lonza, Switzerland) supplemented with 10% fetal bovine serum (FBS, Gibco, USA) at 37°C in a 5% CO_2-95% air atmospheric condition. When cells were 80–90% confluence, the adherent cells were trypsinized and passaged at a 1:2 ratio. HUVECs in the third-seventh passages were used for experiments.

Human foreskin fibroblasts (HFFs, a cell line) were obtained from the Cell Bank of the Chinese Academy of Sciences (China). HFFs were cultured α-modified essential medium (α-MEM, Gibco, USA) supplemented with 10% fetal bovine serum (FBS, Gibco, USA) at 37°C in a 5% CO_2-95% air atmospheric. When cells were 80–90% confluence, HFFs were trypsinized and passaged at a 1:2 ratio.

Induction of HUVEC Apoptosis and Isolation of ApoEVs

Induction of HUVEC apoptosis was performed as induction of MSC apoptosis reported by Zhang et al[18] with modifications. Briefly, HUVECs were washed twice with PBS and the culture medium was replaced by EGM supplemented with 250 nM staurosporine (STS, Beyotime, China). After 8 h induction, ApoEVs were isolated from the culture medium using sequential centrifugation. After sequential centrifugation once at 800 g for 10 min and once at 2000 g for 20 min, cell debris and larger vesicles were removed. The supernatant was further collected and centrifuged at 16,000 g for 30 min at 4°C to obtain ApoEVs.

Characterization of Apoptotic HUVECs

For morphology detection, images were captured by an inverted microscope (Olympus, Japan). The apoptosis of HUVECs was further evaluated by TdT-mediated dUTP nick-end labeling (TUNEL) assay and flow cytometry analysis, which was usually used for apoptosis evaluation. For the TUNEL assay, cells were fixed with 4% paraformaldehyde (Biosharp, USA) for 10 min and underwent permeabilization with 0.05% Triton X-100 (Sigma-Aldrich, USA) for 15 min. Then, cells were incubated with TUNEL reagent (Beyotime, China) for 60 min at 37°C. The nuclei were marked by DAPI (C0050, Solarbio, China) for 10 min. Images were captured by confocal microscopy (Olympus FV1000, Japan).

For flow cytometry analysis, cells were trypsinized, centrifugated, and resuspended in the binding buffer. Then, according to the manufacturer's instruction of the Kit (BD, USA), cells were incubated with FITC Annexin V and PI reagent for 15 min at room temperature. After the same volume of the binding buffer was added to stop the reaction, the apoptosis of HUVECs was measured by flow cytometry (BD, USA). The percentage of positive cells was analyzed by FlowJo software (n=3).

Characterization of ApoEVs

For protein concentration analysis, the BCA protein assay kit (KeyGEN BioTECH, China) was used according to the manufacturer's protocol. For size distribution, ApoEVs were resuspended in deionized water and measured in 488 nm laser scatter mode by Nanoparticle Tracking Analysis (NTA, Particle Metrix, Germany). The data was analyzed by ZetaView software 8.02.31. For morphology observation, ApoEVs were loaded onto formvar carbon-coated grids, and negatively stained with aqueous phosphotungstic acid for 60s. Then, images were captured by a transmission electron microscope (TEM, Tecnai G2 F20 S-Twin, USA). For phosphatidylserine (PtdSer) detection, ApoEVs were suspended in 100 μL PBS and 5 μL FITC Annexin V (BD, USA) was added to mark ApoEVs. Images were captured by confocal microscopy (Olympus FV1000, Japan). The apoptosis-specific marker proteins were detected by Western blotting analysis. 50 μg normal HUVECs, Apoptotic HUVECs, or ApoEVs were mixed with 4×loading buffer (Solarbio, China) and boiled for 10 min. Proteins were resolved in 10% or 15% SDS-PAGE gel for 90 min and blotted onto a nitrocellulose membrane. Then, the membrane was incubated with primary antibodies, cleaved caspase-3 (9664, Cell Signaling Technology, USA), caveolin-1 (D161423, Sangon Biotech, China), Fas (ab82419, Abcam, UK), and β-actin (200068-8F0, Zen Bioscience, China) overnight at 4°C. Horseradish peroxidase (HRP) conjugated secondary antibodies were bound to the primary antibodies for 2 h. Finally, High-sig ECL Western Blotting Substrate (Tanon, China) was used to detect protein signals. Images were captured by a Chemidoc imager (Bio-Rad, USA).

ApoEVs Uptake by HUVECs and HFFs

To test whether HUVECs or HFFs could engulf ApoEVs, 5×10^4 HUVECs or HFFs were seeded into confocal dishes. 20 μg ApoEVs, resuspended in 1 mL culture medium, were labeled with 1 μg DiO (V22886, Life Technology, USA) for 30 min at 37°C, reprecipitated with centrifugation once at 16,000 g for 30 min at 4°C. Cells were cultured with DiO-labeled ApoEVs for 24 h. Then, cells were washed twice with PBS, fixed for 10 min with 4%l paraformaldehyde (Biosharp, USA), and underwent permeabilization for 15 min with 0.05% Triton X-100 (Sigma-Aldrich, USA). The cytoskeleton was stained for 20 min with phalloidin (A34055-300U, Invitrogen, USA), and the nuclei were stained for 10 min with DAPI (C0050, Solarbio, China). Images were captured by confocal microscopy (Olympus FV1000, Japan).

The Proliferation of HUVECs and HFFs

To test the proliferative ability of HUVECs and HFFs regulated by ApoEVs, 2×10^3 cells per well were seeded into a 96-well plate. In the ApoEVs groups, a culture medium containing 10μg/mL, 20μg/mL, 30μg/mL, or 40μg/mL ApoEVs was added. Cells treated with a culture medium only were considered as the control group. After 1, 2, 3, 4, and 5 days of treatment, the optical density (OD) value was tested according to the Cell Counting Kit-8 (CCK-8, KeyGEN BioTECH, China) procedure. Briefly, 10 μL CCK8 solution was added to each well and cultured for 1 h at 37°C. Then, the OD value was measured at a wavelength of 450 nm and used to produce growing curves (n=3).

Migration of HUVECs and HFFs

To test the migrative ability of HUVECs and HFFs regulated by ApoEVs, 1×10^5 cells per well were seeded into a 24-well plate. When cells contacted and formed a confluent monolayer, we used pipette tips to scratch lines. Images at this time (0 h) were captured by an inverted microscope (Olympus, Japan). In the ApoEVs groups, we added a culture medium containing 10μg/mL, 20μg/mL, 30μg/mL, or 40μg/mL ApoEVs without any inhibitors. In the control group, cells were added with a culture medium without any inhibitors. After treatment for 24 h, Images were captured by an inverted microscope (Olympus, Japan). The relative migrated area was measured using ImageJ 1.53a software (n=3).

Tube Formation of HUVECs

To test the tube formation of endothelial cells regulated by ApoEVs, In the ApoEVs groups, a culture medium containing 10μg/mL, 20μg/mL, 30μg/mL, or 40μg/mL ApoEVs was added to pretreat HUVECs for 24 h. Cells treated with a culture medium only were considered as the control group. Then, cells were trypsinized, centrifugated, and resuspended in a culture medium. A 96-well plate was coated with 50 μL Matrigel (Corning, USA) and 1×10^4 cells per well were seeded into the plate. After culturing for 3.5 h, images were captured by an inverted microscope (Olympus, Japan). The number of nodes, number of junctions, and total length were analyzed by ImageJ 1.53a software (n=3).

Quantitative Real-Time Polymerase Chain Reaction (qRT-PCR)

To investigate the differentiative ability of HUVECs and HFFs regulated by ApoEVs, cells 1×10^5 cells per well were seeded into a 24-well plate. In the ApoEVs groups, a culture medium containing 10μg/mL, 20μg/mL, 30μg/mL, or 40μg/mL ApoEVs was added. Cells treated with a culture medium only were considered as the control group. The culture medium per well was changed every 2 days to maintain the treatment effect. After 4 days of culturing HUVECs and 10 days of culturing HFFs, cells were trypsinized and centrifugated. The RNAiso Plus (TaKaRa Biotechnology, Japan) was added to isolate the total RNA. The RevertAid First Strand cDNA Synthesis Kit (Thermo Scientific, USA) was used to reverse transcribe RNA into cDNAs. The synthesized cDNAs were amplified with SYBR Premix ExTaq (TaKaRa Biotechnology, Japan) using QuantStudio 6 Flex Real-Time PCR System (Life Technologies, China). The PCR cycling parameters were at 95 °C for 2 min, 44 cycles at 95 °C for 5 s, and at 60 °C for 30s. The results were analyzed by using the $2^{-\Delta\Delta CT}$ relative quantitative method. The relative expression of CD31, vascular endothelial growth factor (VEGF), angiogenin, Col 1, and Col 3 was evaluated with GAPDH as an internal control (n=3). Primer sequences were listed in Supplementary Table S1.

Full-Thickness Skin Wound Model

Sprague Dawley (SD) rats (4-week-old, 75 ± 10 g, n=6) were purchased from Chengdu Dashuo experimental animal Co., Ltd (China). All animal experiments followed the Animal Research: Reporting of in Vivo Experiments (ARRIVE) guidelines and were performed according to protocols approved by the Institutional Animal Care and Use Committee (IACUC) at Sichuan University. Besides, this study was reviewed and approved by the Ethics Committees of the State Key Laboratory of Oral Diseases, West China School of Stomatology, Sichuan University (approval number: WCHSIRB-D-2023-217).

All operations of rats were performed under general anesthesia with pentobarbital sodium. Two circular full-thickness skin wounds (16 mm in diameter) were constructed on the left and right sides of the rat dorsum. 4 μg ApoEVs resuspended in 200 μL PBS (20 μg/mL) were subcutaneously injected around the wounds on the right side as the experimental group, while 200 μL PBS only was subcutaneously injected around the wounds on the left side as the control group. Injections in each group were performed every 3 days until day 15. Digital pictures were taken on day 0, day 3, day 6, day 9, day 12, day 15, and day 45. The relative wound area was measured by ImageJ 1.53a software. Rats were euthanized via rapid cervical dislocation on day 6 and day 45 respectively (n=3).

Hematoxylin and Eosin (H&E) Staining and Masson Staining

To evaluate the structure of wounds and scars, samples were fixed overnight with 4% paraformaldehyde (Biosharp, USA), dehydrated with gradient ethanol, transparent with xylene, and finally embedded with paraffin and cut into 5–6 μm sections. H&E staining (Solarbio, China) was used to visualize the structure of wounds and scars. Masson staining (Baso, China) was used to visualize the collagen fibers.

Immunofluorescence Staining

To further evaluate the types of collagen fibers, the sections of scars on day 45 were blocked for 30 min with 5% bovine serum albumin (BSA, Sigma-Aldrich, USA) and then incubated overnight at 4°C with primary antibodies, Col 1 (ab270993, Abcam, UK) and Col 3 (ab184993, Abcam, UK). Secondary antibodies, goat anti-rabbit 488 (A11008, Invitrogen, USA) and goat anti-rabbit 555 (A21428, Invitrogen, USA), were used to bind to the primary antibodies for 1

h at 37°C. Finally, DAPI (C0050, Solarbio, China) was used to mark the nuclei for 10 min. Fluorescent images were captured by confocal microscopy (Olympus FV1000, Japan). The fluorescence intensity of DAPI, Col 1, and Col 3 was measured using ImageJ 1.53a software. The image was converted to grayscale, a threshold was set, and the density was automatically calculated by the software. The relative fluorescence intensity was determined as the ratio of Col 1/DAPI, Col 3/DAPI, and Col 3/Col 1 (n=3).

Statistical Analysis

Statistical analysis was performed by Microsoft Excel or GraphPad Prism 7 software. Results were presented as mean value ± standard deviation or violin plot. The level of significance was determined by an unpaired two-tailed Student's *t*-test.

Results

Characterization of HUVEC Apoptosis and ApoEVs

We used staurosporine (STS) to induce apoptosis of HUVECs and then isolated ApoEVs using a sequential centrifugation method (Figure 1A). After 8 h of STS induction, HUVECs showed significant morphological changes and apoptotic responses as assessed by TUNEL assay and flow cytometry analysis with FITC Annexin V and PI staining (Figure 1B–E). We used nanoparticle track analysis (NTA) and transmission electron microscopy (TEM) to confirm the morphology and

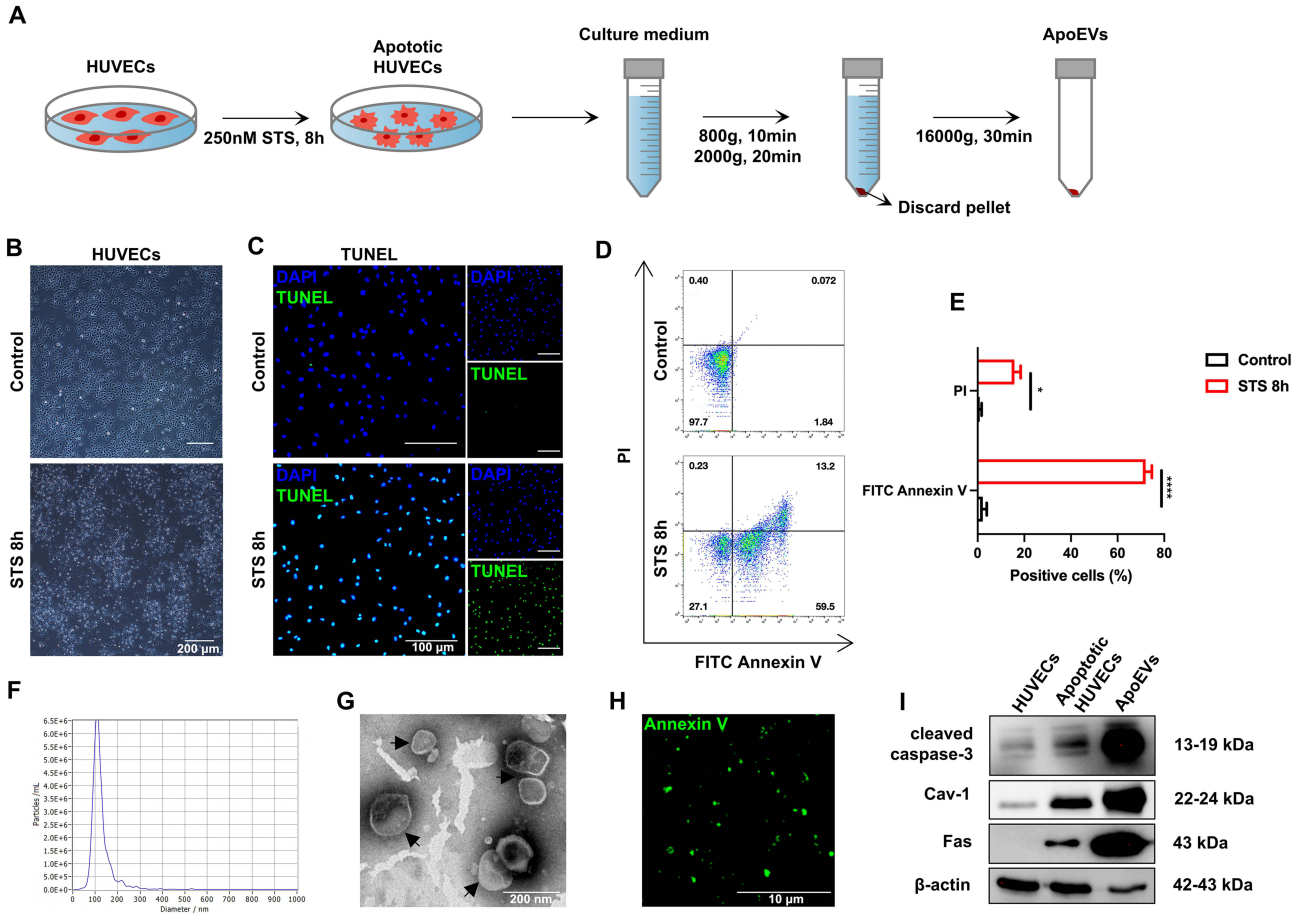

Figure 1 Isolation and characteristics of ApoEVs. (**A**) Schematic view of the process of isolating ApoEVs. Briefly, HUVECs were induced by 250 nM STS for 8 h and then the culture medium was sequentially centrifuged to obtain ApoEVs. (**B**) The morphology of normal and apoptotic HUVECs. Scale bar=200 μm. (**C**) TUNEL analysis of normal and apoptotic HUVECs. Apoptotic cells were indicated by TUNEL-positive cells (green). Scale bar=100 μm. (**D**) Flow cytometry analysis of normal and apoptotic HUVECs. (**E**) Statistic analysis of the percentage of positive cells. (**F**) NTA analysis of the size distribution of ApoEVs. (**G**) TEM analysis of the morphology and size of ApoEVs. Scale bar=200 nm. (**H**) Immunofluorescence staining of ApoEVs. ApoEVs were indicated by an apoptosis-specific surface marker, Ptdser (shown by Annexin V staining, green). (**I**) Western blotting analysis of cleaved caspase 3, Cav 1, Fas, and β-actin expressed in normal HUVECs, apoptotic HUVECs, and ApoEVs. The significance was tested with an unpaired two-tailed Student's *t*-test. (*p<0.05, ****p<0.0001).

size of HUVECs-derived ApoEVs (Figure 1F–G). To further confirm the purity of ApoEVs, we used FITC Annexin V staining to detect the apoptosis-specific marker, phosphatidylserine (PtdSer) (Figure 1H), and used Western blotting analysis to show that ApoEVs expressed high levels of apoptosis-specific markers such as cleaved caspase-3, caveolin- 1 (Cav-1), and Fas (Figure 1I). Besides, ApoEVs expressed low levels of cytoskeleton protein, actin (Figure 1I).

ApoEVs Significantly Promoted the Proliferation, Migration, and Angiogenic Differentiation of HUVECs in vitro

We tried to determine whether ApoEVs derived from apoptotic HUVECs could regulate the biological function of endothelial cells. First, we verified whether HUVECs could engulf ApoEVs. After treatment of ApoEVs for 24 h, fluorescent images showed that phalloidin-labeled HUVECs engulfed a lot of Dio-labeled ApoEVs (Figure 2A). Then, we tested the effect of different concentrations of ApoEVs (10μg/mL, 20μg/mL, 30μg/mL, and 40μg/mL) on the behaviors of HUVECs. In the CCK8 assay, all concentrations of ApoEVs showed a positive effect. 10 μg/mL ApoEVs could considerably promote the growth of HUVECs compared with the control group, and the increase of ApoEVs showed no significantly increased effect on HUVEC proliferation. But importantly, no inhibitory effect was detected for ApoEVs on HUVECs (Figure 2B and C). In the scratch assay, all concentrations of ApoEVs accelerated the migration of HUVECs, but 20 μg/mL was the most effective (Figure 2D and E). To test the effect of ApoEVs on the angiogenic differentiation of HUVECs, HUVECs were pre-treated with different concentrations of ApoEVs. Tube formation assays indicated that ApoEVs could increase the number of nodes, the number of junctions, and the total length. 20 μg/mL and 30 μg/mL were both more effective (Figure 2F and G). To further determine whether the optimal concentration is 20 μg/mL or 30 μg/mL, we also evaluated the expression of angiogenic-related genes (CD31, VEGF, angiogenin) in HUVECs treated with 20 μg/mL and 30 μg/mL ApoEVs and the results indicated that there was no significance between these two concentrations (Figure 2H).

ApoEVs Slightly Promoted the Proliferation and Migration of HFFs in vitro

Since fibroblasts also played an important role in skin wound healing, we examined whether ApoEVs could regulate the behavior of fibroblasts. Similarly, we verified whether recipient HFFs could engulf ApoEVs. After treatment of ApoEVs for 24h, fluorescent images showed that phalloidin-labeled HFFs engulfed Dio-labeled ApoEVs (Figure 3A). Then, 10μg/mL, 20μg/mL, 30μg/mL, and 40μg/mL were added into the culture medium to test their effect on the growth of HFFs. After treating for 4 days, 30μg/mL, and 40μg/mL showed the ability to promote the growth of HFFs. After treatment for 5 days, only 40μg/mL showed the difference between the control group (Figure 3B and C). A scratch assay indicated that 10μg/mL ApoEVs could not promote the migration of HFFs, while higher concentrations (20μg/mL, 30μg/mL, and 40μg/mL) of ApoEVs promote the migration of HFFs (Figure 3D and E). The expression of fibrogenic-related genes in HFFs showed no difference after treatment with ApoEVs (Figure 3F). These findings indicated that ApoEVs could slightly promote the proliferation and migration of HFFs, but could not regulate the fibrogenic differentiation of HFFs.

ApoEVs Increased Wound Closure, Re-Epithelialization, the Formation of Granulation Tissue, and Vascularization in vivo

Full-thickness skin wound models were used to evaluate the effect of ApoEVs on skin regeneration in vivo. Notably, 20μg/mL and 30 μg/mL ApoEVs from HUVECs showed a similar effect on the proliferation, migration, and angiogenic differentiation of HUVECs (Figure 2). Therefore, the concentration of 20 μg/mL was used as a work concentration in the follow-up study. Skin defects with a diameter of 16 mm were constructed on the left and right sides of the rat dorsum, respectively. ApoEVs suspended in PBS were injected into the right side as the experimental group, while PBS only was injected into the left side as the control group (Figure 4A). The digital pictures (Figure 4B) and pattern diagrams (Figure 4C) of wounds showed that on day 15, skin wounds in the ApoEVs group healed; in contrast, skin wounds in the control group did not. The semiquantitative measure showed treatment with ApoEVs increased the wound closure rate from 6 days to 15 days (Figure 4D).

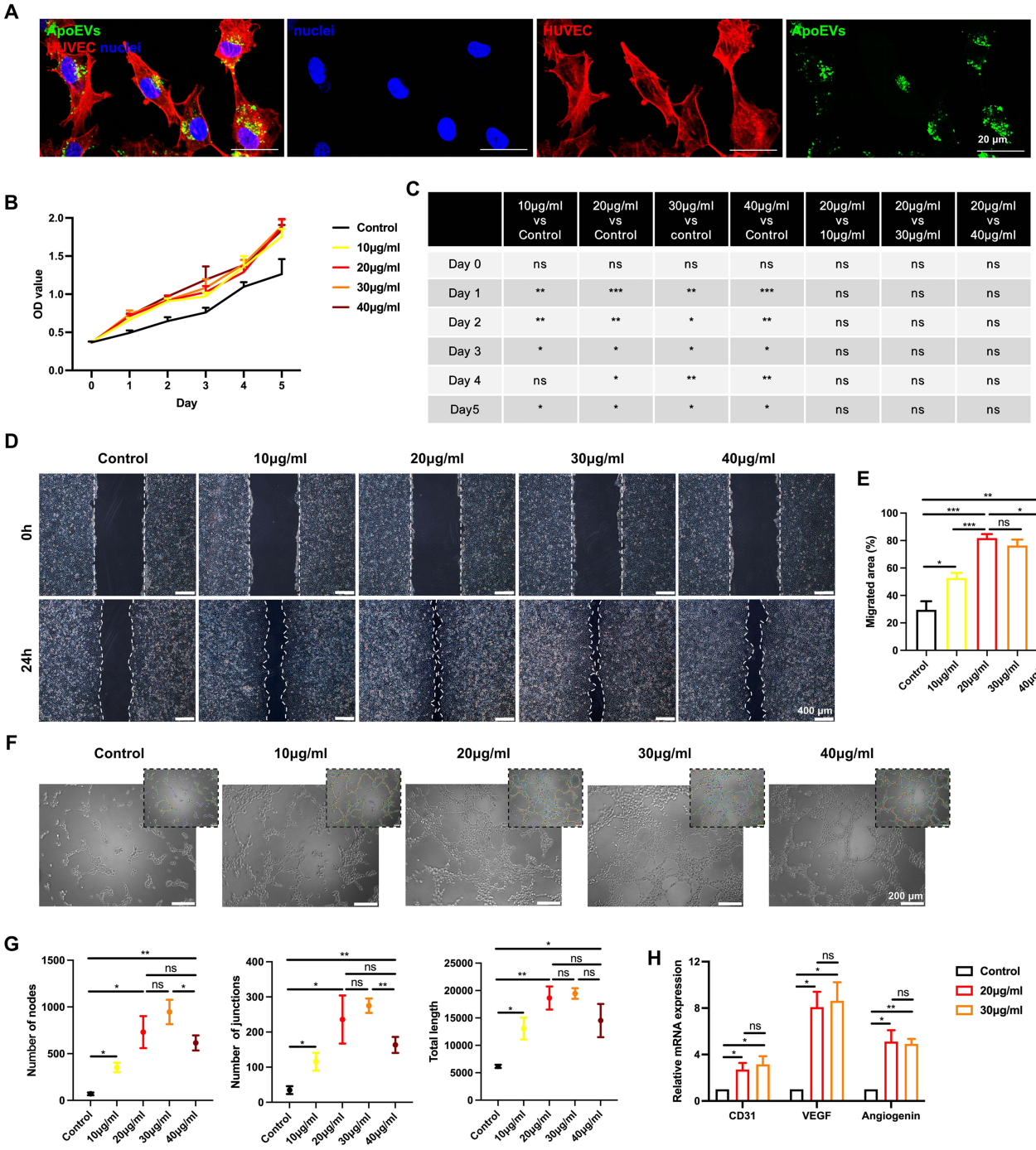

Figure 2 The effect of ApoEVs on the function of HUVECs in vitro. (**A**) Immunofluorescence staining of Dio-labeled ApoEVs (green) engulfed by HUVECs (red). Scale bar=20 μm. (**B** and **C**) CCK-8 analysis of the effect of different concentrations of ApoEVs on the proliferation of HUVECs. (**D**) Scratch analysis of the effect of different concentrations of ApoEVs on the migration of HUVECs. Scale bar=400 μm. (**E**) Statistic analysis of migrated area (n=3). (**F**) Tube formation analysis of the effect of different concentrations of ApoEVs on the angiogenesis of HUVECs. Scale bar=200 μm. (**G**) Statistic analysis of the number of nodes, number of junctions, and total length. (**H**) qRT-PCR analysis of the difference between 20 μg/mL and 30 μg/mL ApoEVs on the angiogenic differentiation of HUVECs. The significance was tested with an unpaired two-tailed Student's *t*-test. (^{ns}p>0.05, *p<0.05, **p<0.01, ***p<0.001).

During the proliferative phase of wound healing, granulation tissue is formed concurrently with re-epithelialization and vascularization. To visualize these structures, skin wounds were collected on day 6. In H&E-stained images, we used black inverted triangles to point out the edge of re-epithelization (Figure 4E). The area of re-epithelialization was increased by ApoEVs (Figure 4F). H&E staining (Figure 4G) and Masson staining (Figure 4H) both indicated that wounds treated with ApoEVs

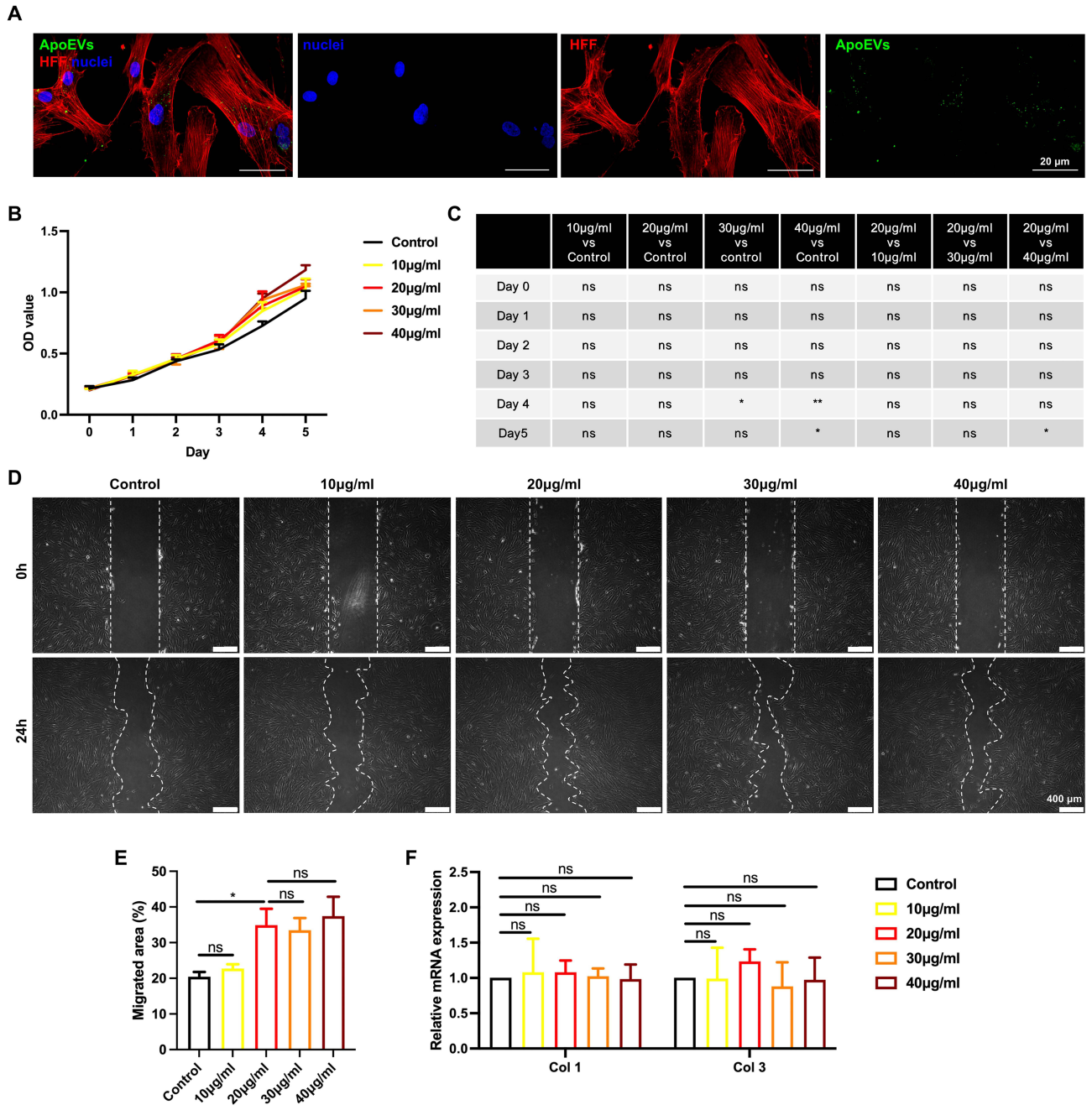

	10μg/ml vs Control	20μg/ml vs Control	30μg/ml vs control	40μg/ml vs Control	20μg/ml vs 10μg/ml	20μg/ml vs 30μg/ml	20μg/ml vs 40μg/ml
Day 0	ns	ns	ns	ns	ns	ns	ns
Day 1	ns	ns	ns	ns	ns	ns	ns
Day 2	ns	ns	ns	ns	ns	ns	ns
Day 3	ns	ns	ns	ns	ns	ns	ns
Day 4	ns	ns	*	**	ns	ns	ns
Day5	ns	ns	ns	*	ns	ns	*

Figure 3 The effect of ApoEVs on the function of HFFs in vitro. (**A**) Immunofluorescence staining of Dio-labeled ApoEVs (green) engulfed by HFFs (red). Scale bar=20 μm. (**B** and **C**) CCK-8 analysis of the effect of different concentrations of ApoEVs on the proliferation of HFFs. (**D**) Scratch analysis of the effect of different concentrations of ApoEVs on the migration of HFFs. Scale bar=400 μm. (**E**) Statistic analysis of migrated area (n=3). (**F**) qRT-PCR analysis of the effect of different concentrations of ApoEVs on the fibrogenic differentiation of HFFs. The significance was tested with an unpaired two-tailed Student's *t*-test. (^{ns}p>0.05, *p<0.05, **p<0.01).

showed a significantly higher thickness of granulation tissue formation (Figure 4I) and more blood vessel regeneration (Figure 4J) than the control group. These findings confirmed the function of ApoEVs in increasing the wound closure rate, re-epithelialization, the formation of granulation tissue, and vascularization.

ApoEVs Reduced Scar Formation in vivo

To assess the formation of scars, we collected healed skins on day 45 and made sections for subsequent staining. Based on digital pictures and pattern diagrams, we found that the relative scar area was reduced by ApoEVs (Figure 5A–C).

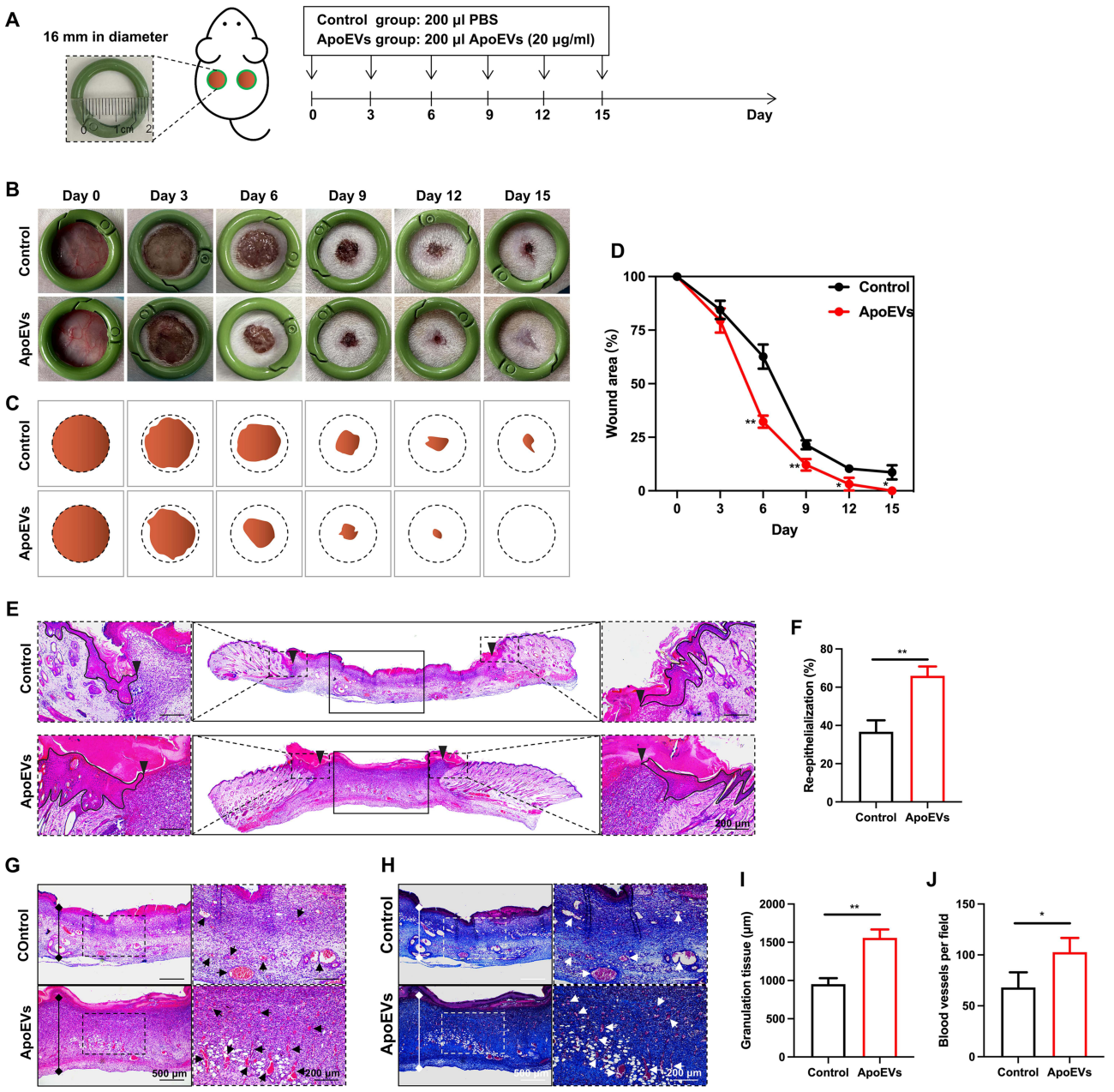

Figure 4 The effect of ApoEVs on wound closure, re-epithelialization, the formation of granulation tissue, and vascularization in vivo. (**A**) Schematic view of the experimental process in vivo. (**B**) Digital pictures of wounds on day 0, day 3, day 6, day 9, day 12, and day 16. The inner diameter of the ring=16 mm. (**C**) Pattern diagrams of wounds at each time point. (**D**) Statistic analysis of the wound closure rate (n=3). (**E**) H&E staining of wounds on day 6. The black inverted triangles pointed out the edge of re-epithelialization. The black lines pointed out the area of the regenerated epidermis. Scale bar=200 μm. (**F**) Statistic analysis of the re-epithelialization rate (n=3). (**G**) H&E staining and (**H**) Masson staining of granulation tissue on day 6. The solid lines with stops represented the thickness of granulation tissue. The arrows pointed out the blood vessels. Scale bar (left)=500 μm. Scale bar (right)=200 μm. (**I**) Statistic analysis of granulation tissue thickness (n=3). (**J**) Statistic analysis of the number of blood vessels per field of view (scale bar=200 μm, n=3). The significance was tested with an unpaired two-tailed Student's *t*-test. (*p<0.05, **p<0.01).

Images with H&E staining also indicated that the scar was narrower in the ApoEVs group than that in the control group (Figure 5D–F). Masson staining indicated that fibers were the main component of scars, so we further performed immunofluorescence staining on these fibers to distinguish different types (Figure 5D and E). The relative fluorescence density (Col 1/DAPI) showed no difference between the control group and the ApoEVs group (Figure 5G). The relative fluorescence density (Col 3/DAPI) was higher in the ApoEVs group than that in the blank group (Figure 5G). The relative fluorescence density of Col 3/Col 1 was increased by ApoEVs (Figure 5G), which was related to the reduction of scar and the increase of skin softness. These findings confirmed that ApoEVs could decrease scar formation.

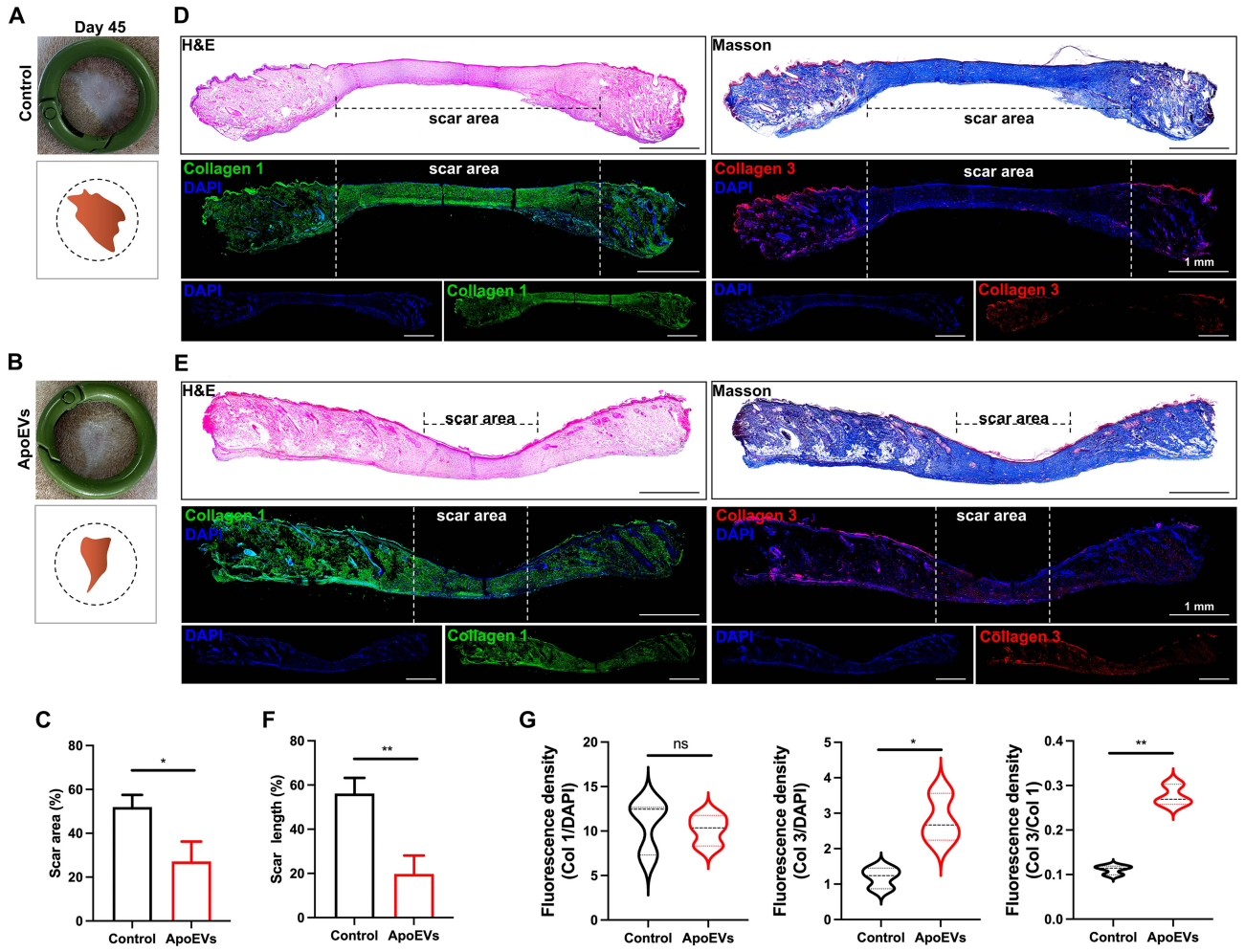

Figure 5 The effect of ApoEVs on scar formation in vivo. (**A** and **B**) Digital pictures and pattern diagrams of scars on day 45. The inner diameter of the ring=16 mm. (**C**) Statistic analysis of the scar area (n=3). (**D** and **E**) H&E staining, Masson staining, and immunofluorescence staining (Col 1 and Col 3) of scars on day 45. The dotted line pointed out the edge of the scars. Scale bar=1 mm. (**F**) Statistic analysis of the percentage of scar length (n=3). (**G**) Statistic analysis of relative fluorescence density (Col 1/DAPI, Col 3/DAPI, Col 3/Col 1) (n=3). The significance was tested with an unpaired two-tailed Student's *t*-test. ($^{ns}p>0.05$, $^{*}p<0.05$, $^{**}p<0.01$).

Discussion

Apoptosis, which is the programmed cell death, occurs daily to ensure cell turnover and maintain tissue homeostasis.[34–36] Efficient removal of apoptotic cells is necessary to prevent further damage to healthy tissue.[37] Apoptotic cells go through a series of biological events, including blebbing, cell shrinkage, nuclear fragmentation, chromatin condensation, and chromosomal DNA fragmentation, leading to the formation of ApoEVs. ApoEVs contain various cellular components such as nucleic acids, proteins, and lipids.[18,38] These ApoEVs are ultimately cleared by different types of phagocytes, including professional, non-professional, and specialized phagocytes, which recognize "Find-Me" signals that promote the engulfment process.[37,39,40] Apoptosis has also gained attention in cell transplantation, as transplanted MSCs undergo extensive apoptosis shortly after injection.[13,22,41,42] Direct delivery of apoptotic MSCs or ApoEVs has shown to be more effective than viable MSCs in disease treatment.[14,15] Additionally, apoptosis of terminally differentiated somatic cells, compared to young cells like stem cells, may better mimic physiological conditions. Therefore, there is a growing focus on apoptosis in current studies.

Most previous studies induced apoptosis of cells by using staurosporine (STS).[18–21,24,43–46] STS has been reported to activate caspase 3 and inhibit cells from entering the G1 or G2 phase of the cell cycle, thereby inducing apoptosis. In this study, we also chose STS as it is commonly used and has been proven effective. Other substances such as Metronidazole[47] and H_2O_2[18,48] have also been found to induce apoptosis in stem cells. Additionally, non-chemical

methods like UVC light,[49] high hydrostatic pressure (HHP),[50] and starvation[18] have shown effectiveness in inducing apoptosis in stem cells. However, further research is needed to investigate the effectiveness of disease treatment using ApoEVs induced by these methods, particularly non-chemical approaches that do not involve the use of exogenous chemical reagents.

In the process of inducing cell apoptosis, there are variations in the apoptosis process among thousands of cells. To prevent excessive cells from entering the late stage of apoptosis, most studies choose to terminate induction when the proportion of apoptosis reaches 60–90%,[16,19,48] which is similar to our termination timing. However, even though the vesicles show basic characteristics of apoptotic vesicles, such as positive expression of PtdSer, Caspase-3, Cav1, and Fas, normal extracellular vesicles are inevitably mixed in. Yang et al conducted a comparison between ApoEVs and normal EVs in diabetic skin wound healing and found no difference.[51] However, comprehensive comparisons like this are rarely conducted. Similarly, further research is needed to understand the composition and function of apoptotic and normal vesicles derived from HUVECs.

The skin serves as the body's primary defense mechanism, making it susceptible to damage.[52] The process of classical cutaneous wound healing is intricate. Initially, a clot forms to seal the wound. The repair and regeneration of the area then occur, involving the introduction of fibroblasts, capillaries, and immune cells into the clot, which leads to the formation of granulation tissue. Eventually, the wound edges come together, and the epidermal layer covers the wound surface. The formation of multilayered skin relies on a delicate balance between various cellular activities, including proliferation, migration, differentiation, and apoptosis.[52,53] Angiogenesis, the development of new blood vessels, plays a crucial role in the regeneration of damaged skin.[1,53] It involves the proliferation, migration, and branching of endothelial cells to form new blood vessels. In previous years, researchers have explored the potential of using of endothelial cells,[3–7,54] endothelial cells-derived conditioned medium,[27] and exosomes[28,31,55] for vascularization in tissue repair and regeneration. In this study, ApoEVs isolated from HUVECs were found to be engulfed by HUVECs, leading to a significant enhancement in the migration and angiogenesis abilities of HUVECs within one day of treatment. Moreover, the proliferation of HUVECs was also significantly enhanced by ApoEVs within five days. In vivo experiments also indirectly confirmed the angiogenic function of ApoEVs, as more blood vessel formation was observed in the ApoEVs group. These findings suggest that ApoEVs promote cutaneous wound healing at least partially by regulating the angiogenesis of endothelial cells.

Fibroblasts, which are present throughout the connective tissue of every organ system, play a crucial role in wound healing. They deposit and remodel the extracellular matrix (ECM) and are responsible for ECM synthesis, proliferation, and migration, which are fundamental processes in wound healing.[56–59] Furthermore, fibroblast-mediated collagen synthesis and deposition differ between fetal and adult wounds. While both types of wounds contain collagen types I and III, fetal wounds have a higher ratio of type III to type I collagen. The presence of collagen type III improves the softness and elasticity of the skin, which decreases as the fetus develops. This transition from scarless to fibrotic repair correlates with changes in collagen organization.[60,61] Previous studies found adipose tissue-derived ApoEVs could directly increase the ratio of type III to type I collagen in fibroblasts and promote skin wound healing.[25] The effects of HUVECs-derived ApoEVs on fibroblasts were investigated in this study. In vitro experiments revealed that ApoEVs could slightly promote the proliferation and migration of fibroblasts. However, no significant changes were observed in the expression of collagen type I and collagen type III. It is worth noting that fibroblasts, as non-professional phagocytes, may have limited phagocytic abilities compared to endothelial cells. Therefore, they might not engulf and process large amounts of HUVECs-derived ApoEVs. However, the in vivo results showed an increased ratio of type III to type I collagen in response to ApoEVs. The complexity of the wound healing process may be regulated by the wound microenvironment, rather than just direct regulation by ApoEVs. ApoEVs may have created a favorable microenvironment for fibroblast differentiation by regulating the behavior of other cells. However, further research is needed to investigate and confirm this assumption and possibility.

Furthermore, ApoEVs are one type of extracellular vesicles, containing various components such as proteins, nucleic acids, and lipids. These components are believed to have an important role in disease treatment. For example, Zhu et al discovered that ApoEVs derived from human bone marrow mesenchymal stem cells (hBMMSCs) enriched in miR1324 could attenuate bone loss.[43] Qu et al found that ApoEVs derived from human embryonic stem cells (ESCs) promoted

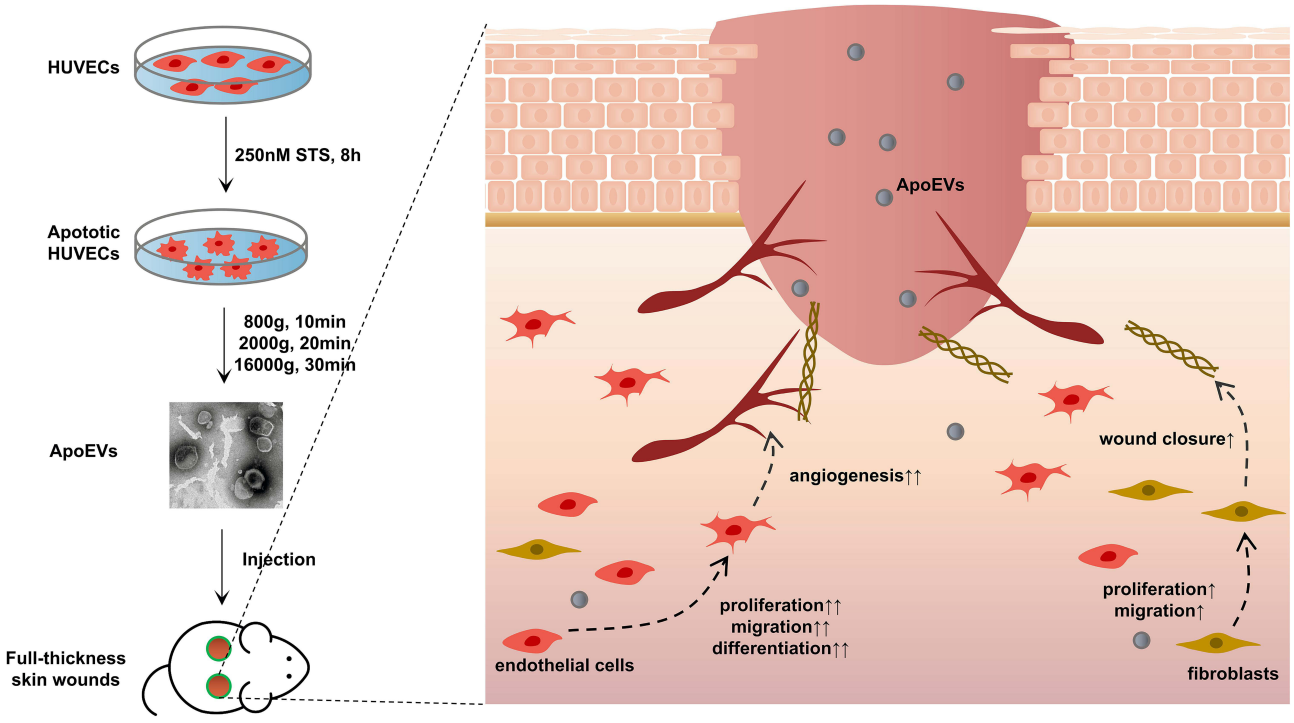

Figure 6 Conclusion. HUVECs-derived ApoEVs promoted skin wound healing.

mouse skin wound healing by transferring SOX2 into skin MSCs.[23] Although we have confirmed that ApoEVs derived from HUVECs showed a significant effect on promoting angiogenesis, the explanation of its mechanism is limited. Further investigation is needed to identify the specific components of HUVECs-derived ApoEVs that play a crucial role in modulating angiogenesis.

Conclusion

In summary, the study demonstrated that an appropriate dosage of ApoEVs derived from HUVECs has the potential to promote full-thickness wound healing by enhancing the proliferation, migration, and angiogenesis of endothelial cells (Figure 6). This finding provides a novel and promising approach to enhancing tissue regeneration through the stimulation of angiogenesis and deepens the understanding of from death to regeneration.

Author Contributions

All authors made a significant contribution to the work reported, whether that is in the conception, study design, execution, acquisition of data, analysis and interpretation, or in all these areas; took part in drafting, revising or critically reviewing the article; gave final approval of the version to be published; have agreed on the journal to which the article has been submitted; and agree to be accountable for all aspects of the work.

Funding

This work was financially supported by National Nature Science Foundations of China (Nos. 82271016, 82071164), Research and Development Program (West China Hospital of Stomatology, Sichuan University) (No. RD-03-202310), and Sichuan Science and Technology Program (No. 2023ZYD0109).

Disclosure

The authors report no conflicts of interest in this work.

References

1. Nosrati H, Aramideh Khouy R, Nosrati A, et al. Nanocomposite scaffolds for accelerating chronic wound healing by enhancing angiogenesis. *J Nanobiotechnology*. 2021;19(1):1. doi:10.1186/s12951-020-00755-7
2. Gurtner GC, Werner S, Barrandon Y, Longaker MT. Wound repair and regeneration. *Nature*. 2008;453(7193):314–321. doi:10.1038/nature07039
3. Zhang W, Wray LS, Rnjak-Kovacina J, et al. Vascularization of hollow channel-modified porous silk scaffolds with endothelial cells for tissue regeneration. *Biomaterials*. 2015;56:68–77. doi:10.1016/j.biomaterials.2015.03.053
4. Suss PH, Capriglione LG, Barchiki F, et al. Direct intracardiac injection of umbilical cord-derived stromal cells and umbilical cord blood-derived endothelial cells for the treatment of ischemic cardiomyopathy. *Exp Biol Med*. 2015;240(7):969–978. doi:10.1177/1535370214565077
5. Kaigler D, Krebsbach PH, Wang Z, West ER, Horger K, Mooney DJ. Transplanted endothelial cells enhance orthotopic bone regeneration. *J Dent Res*. 2006;85(7):633–637. doi:10.1177/154405910608500710
6. Abaci HE, Guo Z, Coffman A, et al. Human skin constructs with spatially controlled vasculature using primary and iPSC-derived endothelial cells. *Adv Healthc Mater*. 2016;5(14):1800–1807. doi:10.1002/adhm.201500936
7. Bak S, Ahmad T, Lee YB, Lee JY, Kim EM, Shin H. Delivery of a cell patch of cocultured endothelial cells and smooth muscle cells using thermoresponsive hydrogels for enhanced angiogenesis. *Tissue Eng Part A*. 2016;22(1–2):182–193. doi:10.1089/ten.tea.2015.0124
8. Volarevic V, Markovic BS, Gazdic M, et al. Ethical and safety issues of stem cell-based therapy. *Int J Med Sci*. 2018;15(1):36–45. doi:10.7150/ijms.21666
9. Bian D, Wu Y, Song G, Azizi R, Zamani A. The application of mesenchymal stromal cells (MSCs) and their derivative exosome in skin wound healing: a comprehensive review. *Stem Cell Res Ther*. 2022;13(1):24. doi:10.1186/s13287-021-02697-9
10. Zou J, Yang W, Cui W, et al. Therapeutic potential and mechanisms of mesenchymal stem cell-derived exosomes as bioactive materials in tendon-bone healing. *J Nanobiotechnology*. 2023;21(1):14. doi:10.1186/s12951-023-01778-6
11. Fu Y, Sui B, Xiang L, et al. Emerging understanding of apoptosis in mediating mesenchymal stem cell therapy. *Cell Death Dis*. 2021;12(6):596. doi:10.1038/s41419-021-03883-6
12. Gregory CD, Rimmer MP. Extracellular vesicles arising from apoptosis: forms, functions, and applications. *J Pathol*. 2023;260(5):592–608. doi:10.1002/path.6138
13. Li M, Xing X, Huang H, et al. BMSC-derived ApoEVs promote craniofacial bone repair via ROS/JNK signaling. *J Dent Res*. 2022;101(6):714–723. doi:10.1177/00220345211068338
14. Chang CL, Leu S, Sung HC, et al. Impact of apoptotic adipose-derived mesenchymal stem cells on attenuating organ damage and reducing mortality in rat sepsis syndrome induced by cecal puncture and ligation. *J Transl Med*. 2012;10(1):244. doi:10.1186/1479-5876-10-244
15. Chen HH, Lin KC, Wallace CG, et al. Additional benefit of combined therapy with melatonin and apoptotic adipose-derived mesenchymal stem cell against sepsis-induced kidney injury. *J Pineal Res*. 2014;57(1):16–32. doi:10.1111/jpi.12140
16. Ye Q, Xu H, Liu S, et al. Apoptotic extracellular vesicles alleviate Pg-LPS induced inflammation of macrophages via AMPK/SIRT1/NF-κB pathway and inhibit adjacent osteoclast formation. *J Periodontol*. 2022;93(11):1738–1751. doi:10.1002/JPER.21-0657
17. Ou Q, Tan L, Shao Y, et al. Electrostatic charge-mediated apoptotic vesicle biodistribution attenuates sepsis by switching neutrophil NETosis to apoptosis. *Small*. 2022;18(20):e2200306. doi:10.1002/smll.202200306
18. Zhang X, Tang J, Kou X, et al. Proteomic analysis of MSC-derived apoptotic vesicles identifies Fas inheritance to ameliorate haemophilia a via activating platelet functions. *J Extracell Vesicles*. 2022;11(7). doi:10.1002/jev2.12240
19. Ma L, Chen C, Liu D, et al. Apoptotic extracellular vesicles are metabolized regulators nurturing the skin and hair. *Bioact Mater* 2023;19:626–641. doi:10.1016/j.bioactmat.2022.04.022
20. Wang J, Cao Z, Wang P, et al. Apoptotic extracellular vesicles ameliorate multiple myeloma by restoring fas-mediated apoptosis. *ACS nano*. 2021;15(9):14360–14372. doi:10.1021/acsnano.1c03517
21. Zheng C, Sui B, Zhang X, et al. Apoptotic vesicles restore liver macrophage homeostasis to counteract type 2 diabetes. *J Extracell Vesicles*. 2021;10(7):e12109. doi:10.1002/jev2.12109
22. Liu H, Liu S, Qiu X, et al. Donor MSCs release apoptotic bodies to improve myocardial infarction via autophagy regulation in recipient cells. *Autophagy*. 2020;16(12):2140–2155. doi:10.1080/15548627.2020.1717128
23. Qu Y, He Y, Meng B, et al. Apoptotic vesicles inherit SOX2 from pluripotent stem cells to accelerate wound healing by energizing mesenchymal stem cells. *Acta Biomater*. 2022;149:258–272. doi:10.1016/j.actbio.2022.07.009
24. Li Z, Wu M, Liu S, et al. Apoptotic vesicles activate autophagy in recipient cells to induce angiogenesis and dental pulp regeneration. *Mol Ther*. 2022;30(10):3193–3208. doi:10.1016/j.ymthe.2022.05.006
25. Dong J, Wu B, Tian W. Preparation of apoptotic extracellular vesicles from adipose tissue and their efficacy in promoting high-quality skin wound healing. *Int J Nanomed*. 2023;18:2923–2938. doi:10.2147/IJN.S411819
26. Liu J, Qiu X, Lv Y, et al. Apoptotic bodies derived from mesenchymal stem cells promote cutaneous wound healing via regulating the functions of macrophages. *Stem Cell Res Ther*. 2020;11(1):507. doi:10.1186/s13287-020-02014-w
27. Castelli G, Parolini I, Cerio AM, et al. Conditioned medium from human umbilical vein endothelial cells markedly improves the proliferation and differentiation of circulating endothelial progenitors. *Blood Cells Mol Dis*. 2016;61:58–65. doi:10.1016/j.bcmd.2016.07.007
28. Liu W, Feng Y, Wang X, et al. Human umbilical vein endothelial cells-derived exosomes enhance cardiac function after acute myocardial infarction by activating the PI3K/AKT signaling pathway. *Bioengineered*. 2022;13(4):8850–8865. doi:10.1080/21655979.2022.2056317
29. Ma T, Hu Y, Guo Y, Zhang Q. Human umbilical vein endothelial cells-derived microRNA-203-containing extracellular vesicles alleviate non-small-cell lung cancer progression through modulating the DTL/p21 axis. *Cancer Gene Ther*. 2022;29(1):87–100. doi:10.1038/s41417-020-00292-3
30. Wong PF, Tong KL, Jamal J, Khor ES, Lai SL, Mustafa MR. Senescent HUVECs-secreted exosomes trigger endothelial barrier dysfunction in young endothelial cells. *Excli J*. 2019;18:764–776. doi:10.17179/excli2019-1505
31. Yang J, Hu Y, Wang L, Sun X, Yu L, Guo W. Human umbilical vein endothelial cells derived-exosomes promote osteosarcoma cell stemness by activating Notch signaling pathway. *Bioengineered*. 2021;12(2):11007–11017. doi:10.1080/21655979.2021.2005220
32. Zhang YZ, Liu F, Song CG, et al. Exosomes derived from human umbilical vein endothelial cells promote neural stem cell expansion while maintain their stemness in culture. *Biochem Biophys Res Commun*. 2018;495(1):892–898. doi:10.1016/j.bbrc.2017.11.092

33. Zhong Y, Luo L. Exosomes from human umbilical vein endothelial cells ameliorate ischemic injuries by suppressing the RNA component of mitochondrial RNA-processing endoribonuclease via the induction of miR-206/miR-1-3p levels. *Neuroscience*. 2021;476:34–44.
34. Kerr JF, Wyllie AH, Currie AR. Apoptosis: a basic biological phenomenon with wide-ranging implications in tissue kinetics. *Br J Cancer*. 1972;26 (4):239–257. doi:10.1038/bjc.1972.33
35. Elmore S. Apoptosis: a review of programmed cell death. *Toxicol Pathol*. 2007;35(4):495–516. doi:10.1080/01926230701320337
36. Kopeina GS, Zhivotovsky B. Programmed cell death: past, present and future. *Biochem Biophys Res Commun*. 2022;633:55–58. doi:10.1016/j.bbrc.2022.09.022
37. Elliott MR, Ravichandran KS. The dynamics of apoptotic cell clearance. *Dev Cell*. 2016;38(2):147–160.
38. Atkin-Smith GK, Tixeira R, Paone S, et al. A novel mechanism of generating extracellular vesicles during apoptosis via a beads-on-a-string membrane structure. *Nat Commun*. 2015;6(1):7439. doi:10.1038/ncomms8439
39. Arandjelovic S, Ravichandran KS. Phagocytosis of apoptotic cells in homeostasis. *Nat Immunol*. 2015;16(9):907–917.
40. Caruso S, Poon IKH. Apoptotic cell-derived extracellular vesicles: more than just debris. *Front Immunol*. 2018;9:1486.
41. Liu S, Jiang L, Li H, et al. Mesenchymal stem cells prevent hypertrophic scar formation via inflammatory regulation when undergoing apoptosis. *J Invest Dermatol*. 2014;134(10):2648–2657. doi:10.1038/jid.2014.169
42. Lee RH, Pulin AA, Seo MJ, et al. Intravenous hMSCs improve myocardial infarction in mice because cells embolized in lung are activated to secrete the anti-inflammatory protein TSG-6. *Cell Stem Cell*. 2009;5(1):54–63. doi:10.1016/j.stem.2009.05.003
43. Zhu Y, Yang K, Cheng Y, et al. Apoptotic vesicles regulate bone metabolism via the miR1324/SNX14/SMAD1/5 signaling axis. *Small*. 2023;19 (16):e2205813. doi:10.1002/smll.202370106
44. Ye Q, Qiu X, Wang J, et al. MSCs-derived apoptotic extracellular vesicles promote muscle regeneration by inducing Pannexin 1 channel-dependent creatine release by myoblasts. *Int J Oral Sci*. 2023;15(1):7.
45. Wang Y, Jing L, Lei X, et al. Umbilical cord mesenchymal stem cell-derived apoptotic extracellular vesicles ameliorate cutaneous wound healing in type 2 diabetic mice via macrophage pyroptosis inhibition. *Stem Cell Res Ther*. 2023;14(1):257. doi:10.1186/s13287-023-03490-6
46. Wang R, Hao M, Kou X, et al. Apoptotic vesicles ameliorate lupus and arthritis via phosphatidylserine-mediated modulation of T cell receptor signaling. *Bioact Mater*. 2023;25:472–484.
47. Brock CK, Wallin ST, Ruiz OE, et al. Stem cell proliferation is induced by apoptotic bodies from dying cells during epithelial tissue maintenance. *Nat Commun*. 2019;10(1):1044. doi:10.1038/s41467-019-09010-6
48. You Y, Xu J, Liu Y, et al. Tailored apoptotic vesicle delivery platform for inflammatory regulation and tissue repair to ameliorate ischemic stroke. *ACS Nano*. 2023;17(9):8646–8662. doi:10.1021/acsnano.3c01497
49. Xin L, Wei C, Tong X, et al. In situ delivery of apoptotic bodies derived from mesenchymal stem cells via a hyaluronic acid hydrogel: a therapy for intrauterine adhesions. *Bioact Mater*. 2022;12:107–119. doi:10.1016/j.bioactmat.2021.10.025
50. Le TM, Morimoto N, Ntm L, et al. Ex vivo induction of apoptotic mesenchymal stem cell by high hydrostatic pressure. *Stem Cell Rev Rep*. 2021;17 (2):662–672. doi:10.1007/s12015-020-10071-0
51. Yang J, Zhang X, Wang G, et al. ApoSEVs-mediated modulation of versatile target cells promotes diabetic wound healing: unveiling a promising strategy. *Int J Nanomed*. 2023;18:6955–6977. doi:10.2147/IJN.S436350
52. Rodrigues M, Kosaric N, Bonham C, Gurtner G. Wound Healing: a Cellular Perspective. *Physiol Rev*. 2019;99(1):665–706. doi:10.1152/physrev.00067.2017
53. Dong J, Wu B, Tian W. How to maximize the therapeutic effect of exosomes on skin wounds in diabetes mellitus: review and discussion. *Front Endocrino*. 2023;14:1146991. doi:10.3389/fendo.2023.1146991
54. Sueyama Y, Kaneko T, Ito T, Kaneko R, Okiji T. Implantation of endothelial cells with mesenchymal stem cells accelerates dental pulp tissue regeneration/healing in pulpotomized rat molars. *J Endod*. 2017;43(6):943–948. doi:10.1016/j.joen.2017.01.035
55. Li L, Mu J, Zhang Y, et al. Stimulation by exosomes from hypoxia preconditioned human umbilical vein endothelial cells facilitates mesenchymal stem cells angiogenic function for spinal cord repair. *ACS Nano*. 2022;16(7):10811–10823. doi:10.1021/acsnano.2c02898
56. Rowlatt U. Intrauterine wound healing in a 20 week human fetus. *Virchows Arch Pathol Anat Histol*. 1979;381(3):353–361. doi:10.1007/BF00432477
57. Willyard C. Unlocking the secrets of scar-free skin healing. *Nature*. 2018;563(7732):S86–S88. doi:10.1038/d41586-018-07430-w
58. Chang HY, Chi JT, Dudoit S, et al. Diversity, topographic differentiation, and positional memory in human fibroblasts. *Proc Natl Acad Sci U S A*. 2002;99(20):12877–12882. doi:10.1073/pnas.162488599
59. Lovvorn HN, Cheung DT, Nimni ME, Perelman N, Estes JM, Adzick NS. Relative distribution and crosslinking of collagen distinguish fetal from adult sheep wound repair. *J Pediatr Surg*. 1999;34(1):218–223. doi:10.1016/S0022-3468(99)90261-0
60. Longaker MT, Whitby DJ, Adzick NS, et al. Studies in fetal wound healing, VI. Second and early third trimester fetal wounds demonstrate rapid collagen deposition without scar formation. *J Pediatr Surg*. 1990;25(1):63–68; discussion 68–69. doi:10.1016/S0022-3468(05)80165-4
61. Merkel JR, DiPaolo BR, Hallock GG, Rice DC. Type I and type III collagen content of healing wounds in fetal and adult rats. *Proc Soc Exp Biol Med*. 1988;187(4):493–497. doi:10.3181/00379727-187-42694